Oecologia (2014) 174:699–712
DOI 10.1007/s00442-013-2832-3

PHYSIOLOGICAL ECOLOGY - ORIGINAL RESEARCH

# Fatty acid and stable isotope characteristics of sea ice and pelagic particulate organic matter in the Bering Sea: tools for estimating sea ice algal contribution to Arctic food web production

**Shiway W. Wang · Suzanne M. Budge · Rolf R. Gradinger · Katrin Iken · Matthew J. Wooller**

Received: 28 August 2013 / Accepted: 6 November 2013 / Published online: 26 November 2013


**Abstract** We determined fatty acid (FA) profiles and carbon stable isotopic composition of individual FAs ($\delta^{13}C_{FA}$ values) from sea ice particulate organic matter (i-POM) and pelagic POM (p-POM) in the Bering Sea during maximum ice extent, ice melt, and ice-free conditions in 2010. Based on FA biomarkers, differences in relative composition of diatoms, dinoflagellates, and bacteria were inferred for i-POM versus p-POM and for seasonal succession stages in p-POM. Proportions of diatom markers were higher in i-POM (16:4n-1, 6.6–8.7 %; 20:5n-3, 19.6–25.9 %) than in p-POM (16:4n-1, 1.2–4.0 %; 20:5n-3, 5.5–14.0 %). The dinoflagellate marker 22:6n-3/20:5n-3 was highest in p-POM. Bacterial FA concentration was higher in the bottom 1 cm of sea ice (14–245 μg $L^{-1}$) than in the water column (0.6–1.7 μg $L^{-1}$). Many i-POM $\delta^{13}C_{FA}$ values were higher (up to~10 ‰) than those of p-POM, and i-POM $\delta^{13}C_{FA}$ values increased with day length. The higher i-POM $\delta^{13}C_{FA}$ values are most likely related to the reduced dissolved inorganic carbon (DIC) availability within the semi-closed sea ice brine channel system. Based on a modified Rayleigh equation, the fraction of sea ice DIC fixed in i-POM ranged from 12 to 73 %, implying that carbon was not limiting for primary productivity in the sympagic habitat. These differences in FA composition and $\delta^{13}C_{FA}$ values between i-POM and p-POM will aid efforts to track the proportional contribution of sea ice algal carbon to higher trophic levels in the Bering Sea and likely other Arctic seas.

**Keywords** Compound-specific carbon stable isotope · Biomarkers · Trophic studies · Marine phytoplankton · Arctic

Communicated by Ulrich Sommer.

**Electronic supplementary material** The online version of this article (doi:10.1007/s00442-013-2832-3) contains supplementary material, which is available to authorized users.

S. W. Wang (✉) · R. R. Gradinger · K. Iken · M. J. Wooller
School of Fisheries and Ocean Sciences, Institute of Marine Science, University of Alaska Fairbanks, Fairbanks, AK 99775, USA
e-mail: shiway@gmail.com

S. W. Wang · M. J. Wooller
Alaska Stable Isotope Facility, Water and Environmental Research Center, Institute of Northern Engineering, University of Alaska Fairbanks, Fairbanks, AK 99775, USA

S. M. Budge
Department of Process Engineering and Applied Science, Dalhousie University, Halifax, NS B3J 2X4, Canada

## Introduction

The contribution of ice algae to total primary production in the seasonally ice-covered Bering Sea is estimated to be between 3 and 30 % (McRoy and Goering 1976; R. R. Gradinger, unpublished data). Thus, the quantitative importance of sea ice algae to marine food webs in Arctic seas such as the Bering Sea remains uncertain (Hobson et al. 1995; Søreide et al. 2006; Budge et al. 2008). In the Bering Sea, the timing of sea ice melt determines the timing of spring phytoplankton blooms, the sources of spring primary production (sympagic or pelagic), and the fate of carbon from this primary production to the marine food web (Walsh and McRoy 1986; Hunt et al. 2002, 2011; Hunt and Stabeno 2002). Climate-related changes in the timing of seasonal sea ice cover affect spring primary production patterns (Stabeno et al. 2001, 2010; Hunt and Stabeno 2002), and these changes will likely propagate through the food web to upper trophic levels (Grebmeier

et al. 2006; Bluhm and Gradinger 2008; Leu et al. 2011; Grebmeier 2012). Furthermore, climate-induced changes in the food quality, such as fatty acid (FA) content derived from sympagic and pelagic primary production, could ultimately influence upper trophic levels (Litzow et al. 2006; Leu et al. 2011).

FA profiles and biomarkers of sea ice algae and phytoplankton have been used to understand the feeding ecology of consumers in a wide range of Arctic seas (e.g., Lewis 1969; Falk-Petersen et al. 1998; Auel et al. 2002; Peters et al. 2004; Budge et al. 2007; Mayzaud et al. 2013). Changes in phytoplankton species composition, productivity, physiological state, and amount of living versus decayed material within the marine particulate organic matter (POM) pool can be inferred from variations in FA profiles of POM (Mayzaud et al. 1989; Reuss and Poulsen 2002; Mayzaud et al. 2013). In addition to FA biomarkers, bulk carbon stable isotopic analyses of organisms have been used to examine the feeding ecology of Arctic marine organisms and food webs (e.g., Dehn et al. 2007; Iken et al. 2010; Feder et al. 2011; Weems et al. 2012). In response to increased seasonal light availability (Gradinger et al. 2009) and a carbon-limiting environment of the closed sea ice system (e.g., Fischer 1991; Schubert and Calvert 2001; Kennedy et al. 2002), POM in sea ice (i-POM) has carbon stable isotope values (expressed here as $\delta^{13}C$ values) that are more enriched in $^{13}C$ than pelagic POM (p-POM) (Hobson et al. 1995; Naidu et al. 2000; Schubert and Calvert 2001; Gradinger et al. 2009; Thomas et al. 2010). In a combination of FA and stable isotope analysis methods, carbon stable isotope analysis of specific FAs ($\delta^{13}C_{FA}$ values, e.g., 16:4n-1 and 20:5n-3) in sea ice algae and pelagic phytoplankton have been investigated (Budge et al. 2008). Sea ice algae $\delta^{13}C_{FA}$ values were higher than pelagic phytoplankton, which allowed for the quantitative estimation of the proportional contribution of sympagic and pelagic primary production to consumers in the Arctic (Budge et al. 2008).

The $\delta^{13}C_{FA}$ data from sea ice algae and marine phytoplankton so far have been restricted to the Chukchi Sea region off of Barrow, Alaska (Budge et al. 2008). Furthermore, the temporal and spatial variability of $\delta^{13}C_{FA}$ values from marine algae from high latitudes, and the processes that generate this isotopic variability, are poorly resolved. Elucidating these patterns and processes in the Bering Sea is important to help interpret $\delta^{13}C_{FA}$ values at higher trophic levels as a way of estimating the importance of sea ice algal carbon and pelagic carbon to food web production. Our goals were to characterize the FA profiles and the $\delta^{13}C_{FA}$ values of i-POM and p-POM in the Bering Sea, examine seasonal differences, and determine if there was a correlation between $\delta^{13}C_{FA}$ values and day length (used here as a proxy for light availability). We hypothesize that differences in FA profiles between POM types can be explained by variation in algal taxon composition. In addition, greater seasonal availability of light at the most southerly sea ice locations in the Bering Sea should stimulate the highest levels of sea ice primary production (McRoy and Goering 1974). This high primary production within the sea ice habitat would then lead to a subsequent $^{13}C$ enrichment of individual FAs as a result of decreased isotopic discrimination during photosynthesis in the carbon-limited and closed sympagic habitats.

## Materials and methods

### Sample collection

i-POM and p-POM samples were collected as part of the Bering Sea Ecosystem Study/Bering Sea Integrated Ecosystem Research Program during three major seasonal ice regimes in 2010 based on timing of sea ice conditions in the northern and central portions of the Bering Sea: maximum ice extent (13-28 March; i-POM $n = 12$, p-POM $n = 14$), ice melt (11 May-10 June; i-POM $n = 1$, p-POM $n = 20$), and ice-free conditions (18 June–10 July; p-POM $n = 15$) (Fig. 1). One p-POM sample was taken from a station in the deep basin of the Bering Sea which did not experience ice cover (Fig. 1). Maximum ice extent occurred on 31 March 2010 and all stations on the Bering Sea shelf experienced ice cover between 21 March and 10 April 2010 (Cavalieri et al. 1996; Richter-Menge and Overland 2010). For the determination of i-POM in March 2010, sea ice cores were collected with an ice corer (9 cm inner diameter) and cut into sections of 1–10 cm thickness (Cooper et al. 2013). Data in this study came from samples taken from the bottom 1-cm sections of the sea ice cores, which were completely melted in the dark and filtered on pre-combusted GF/F filters (melted water volumes ranged from 1.8 to 18.5 mL). The i-POM sample taken during ice melt consisted mainly of *Melosira arctica* (K. Iken, personal observation) collected from overturned ice floes. During maximum ice extent p-POM samples were collected at 15 m below the surface. During ice melt and ice-free conditions, samples were collected at the chlorophyll maximum layer between a depth of 5–29 m from the surface. Each p-POM sample was collected from a single Niskin bottle and sample volumes were between 200 and 1,500 mL. The algal composition in p-POM samples taken during ice melt was described for some stations and contained *Thalassiosira* sp., *Nitzschia frigida*, *Fragillariopsis* sp., *Chaetoceros* sp., *Pseudonitzschia* sp., and *Phaeocystis* sp. (K. Iken, personal observation). Samples were filtered using a GF/F filter (pore size 0.7 μm) and

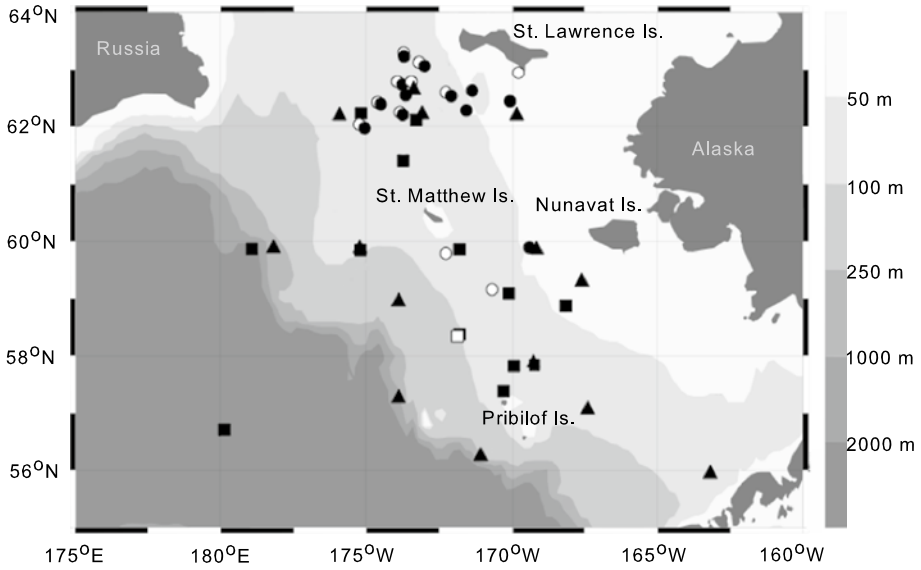


**Fig. 1** Sampling stations for sea ice particulate organic matter (i-POM; *open symbols*) and pelagic POM (p-POM; *shaded symbols*) collected in the Bering Sea in 2010 during maximum ice extent 13–28 March (*circles*; i-POM $n = 12$, p-POM $n = 14$), ice melt between 11 May–10 June (*squares*; i-POM $n = 1$, p-POM $n = 20$), and ice-free (*triangles*; p-POM n = 15) conditions between 18 June and 10 July 2010. Ice conditions were based on the timing of sea ice conditions in the northern and central portions of the overall sampling area

stored in a vial of chloroform at −20 °C until laboratory analysis.

Details for the determination of ice bulk properties are described by Cooper et al. (2013). In short, filters were dried, acid fumed, and analyzed at the Alaska Stable Isotope Facility (ASIF) at the University of Alaska Fairbanks (UAF) for determination of bulk i-POM particulate organic carbon (POC) concentrations and $\delta^{13}C$ values (Cooper et al. 2013). A second set of filters was analyzed for chlorophyll a concentrations using fluorometric determination after extraction in 90 % acetone.

## FA analysis

Lipids were quantitatively extracted from all samples using 2:1 chloroform/methanol at 20–30 parts solvent to sample (Folch et al. 1957; Parrish 1999). FA methyl esters (FAMEs) were prepared using an acidic transesterification (Budge et al. 2006). FAMEs were quantified using temperature-programmed gas chromatography (GC) on a Perkin Elmer Autosystem II Capillary FID gas chromatograph fitted with a 30-m-long × 0.25-mm-internal diameter column coated with 50 % cyanopropyl-methylpolysiloxane (DB-23) and linked to a computerized integration system (Varian Star software). Shorthand nomenclature of *A*:*Bn*-X was used to describe each FAME, where *A* represents the number of carbon atoms, *B* the number of double bonds and X the position of the double bond closest to the terminal methyl group. Approximately 70 FAMEs were identified by comparison of retention times with known standards (Nu Check Prep, Elysian, MN), or using GC-mass spectrometry. Concentrations of each FA were determined from a standard (α-cholestane; Sigma-Aldrich) with a known mass and volume of the sample filtered.

## Compound-specific stable isotope analysis of individual FAs

$\delta^{13}C$ of samples (expressed in per mil—‰) were analyzed from FAME sub-samples by routing the effluent from a GC (Trace GC Ultra; Thermo, Bremen, Germany) through a combustion interface (Finnigan GC combustion III; Thermo) to an isotope ratio mass spectrometer (IRMS) (Thermo Finnigan Delta V; Thermo) at ASIF, UAF. The same GC column and method described above for FID analyses of FAMEs were used to separate the FAMEs for analysis using IRMS. To correct for any influence of carbon from the methyl group added during transesterification and determine any kinetic isotope effects, free FA (FFA) standards 16:0 and 18:0 were transesterified with the same reagents described above. The purity of the FFA was confirmed with thin layer chromatography prior to transesterification and $\delta^{13}C$ values for FFA were determined using an elemental analyzer (Costech ECS4010) routed to an IRMS. The $\delta^{13}C$ values of the respective FAMEs of these FFA that had been transesterified into their respective FAMEs were then also measured using the GC-IRMS system described above. We could not perform this analysis on all the FA examined because most are not commercially available. There was no evidence of a kinetic isotope effect associated with transesterification, which is expected for a reaction that goes to completion (Rieley 1994). The difference between the $\delta^{13}C$ values for FFA and FAME with the same chain length was entirely due to the added methyl group. The proportional contribution of this methyl group to a given FA depends on the chain length. Therefore, an average $\delta^{13}C$ value for this added methyl group was calculated using the following equation:

$$\delta^{13}C = (n+1)[\delta^{13}C_{FAME}] - n[\delta^{13}C_{FFA}],$$

where $n$ is the number of carbon atoms in the FFA (Abrajano et al. 1994). We then calculated an average $\delta^{13}C$ value ($-48.8 \pm 1.3$ ‰, mean ± 1 SD) for the methyl-derived carbon based on the difference between the $\delta^{13}C$ values of the corresponding FFA and their respective FAME. This value was based on three runs each of the C16 and C18 standards, and used to correct our FAME data by applying the above equation. The $\delta^{13}C$ values from the FAMEs were also calibrated using a standard mixture consisting of ethyl and methyl esters of 14:0, 16:0, 18:0, and 20:0 (supplied by Indiana University Stable Isotope Reference Materials) where the coefficient of determination ($r^2$) of the measured versus expected relationship was >0.99. A C16 laboratory standard was analyzed after every ten samples to track analytical error of the GC-IRMS system, which was ≤0.8 ‰ (representing the 1 SD of 14 analyses of the C16 standard interspersed during the samples runs). All $\delta^{13}C$ values are reported relative to Vienna Pee Dee Belemnite using standard notation, where $\delta^{13}C$ (‰) $= [(R_{sample}/R_{standard}) - 1] \times 1{,}000$, and $R$ is the corresponding ratio of $^{13}C/^{12}C$.

## Data analysis

Bray–Curtis similarity matrices and permutational multivariate ANOVA (PERMANOVA; Anderson 2001; McArdle and Anderson 2001) were used to investigate the variation in FA composition, based on 59 FAs present in proportions >0.1 %, between i-POM and p-POM, and seasonal variation within p-POM using PRIMER version 6 (Primer-E). Non-metric multidimensional scaling plots were used to visualize differences among FA profiles of samples. A stress value of <0.1 indicates good fit of the data with little prospect of incorrect interpretation (Clarke 1993). Similarity percentages routines (SIMPER) were performed to determine FAs contributing most to the observed differences. Data were standardized to 100 % and $\log(1 + x)$ transformed prior to analysis.

We examined the proportion of 16:4n-1 and the ratios of 16:1/16:0 and 22:6n-3/20:5n-3 to assess the presence and dominance of diatoms and dinoflagellates in the POM samples (Claustre et al. 1988, 1989; Budge and Parrish 1998). Additionally, the sum of 15:0, 17:0, and the iso- and anteiso-FAs (i-14:0, i-15:0, ai-15:0, i-16:0, i-17:0, and ai-17:0) were used to determine the contribution of bacterial FAs in the POM samples (Budge and Parrish 1998).

$\delta^{13}C_{FA}$ values were determined for 39 FAs. Not all FAs were present in sufficient quantities to be analyzed by GC-IRMS. Out of these 39 FAs, 13 (14:0, 16:0, 16:1n-11/9, 16:1n-7, 16:2n-4, 16:3n-4, 16:4n-1, 18:0, 18:1n-9, 18:2n-6, 18:4n-3, 20:5n-3, and 22:6n-3) were selected for further data analysis because they were identified in most of the samples (63–100 %). FAs 16:1n-11 and 16:1n-9 co-eluted on the GC-IRMS and are referred to here as 16:1n-11/9. Data were not normally distributed, therefore a non-parametric Mann–Whitney $U$-test was used to assess differences in $\delta^{13}C_{FA}$ values of the selected 13 FAs between i-POM and p-POM during maximum ice extent. A Kruskal–Wallis ANOVA was used followed by Bonferroni adjustment for multiple comparisons to test for differences in $\delta^{13}C_{FA}$ values of each FA in p-POM during maximum ice extent, ice melt, and ice-free conditions. Spearman's rank order correlations were performed to examine any correlations between $\delta^{13}C_{FA}$ values of the 13 selected FAs in both i-POM and p-POM samples and day length. A site-specific estimate of light exposure for each station was determined using the U.S. Naval Observatory website http://aa.usno.navy.mil/data/docs/RS_OneDay.php. Significance level α was controlled for multiple comparisons with Holm's sequential Bonferroni adjustments. Spearman's rank order correlations were also performed between day length and POM FA concentrations to determine if FA production increased with light exposure (day length). In addition, correlations were examined between day length, POC concentrations, chlorophyll a concentrations, and bulk $\delta^{13}C$ values measured in i-POM to determine if productivity increased with day length within the closed sea ice system.

We estimated the fraction of source ocean water dissolved inorganic carbon (DIC) used for FA synthesis in sea ice during maximum ice extent using the following Rayleigh equation modified for isotope reaction progress in a closed system (Fry 2006):

$$\delta_{AP} = \delta_{Source} + \Delta * ((1 - f)/f) * \ln(1 - f),$$

where, for each FA, the $\delta^{13}C$ value of the accumulated product ($\delta_{AP}$) is the $\delta^{13}C_{FA}$ value measured from i-POM, $\delta_{Source}$ is the $\delta^{13}C$ value of ocean water DIC, Δ is the difference between the $\delta^{13}C$ value of the $\delta_{Source}$ and instantaneous product (the $\delta^{13}C$ value of product at any instant in time), and $f$ is the fraction or percentage of source (i.e., DIC) reacted. We used two $\delta^{13}C$ values for DIC from previous studies: the mean for surface water of the Pacific Ocean (1.55 ‰) determined by Quay et al. (2003), and the value at the most northerly station in the Pacific Ocean (1.85 ‰) reported by Gruber et al. (1999). p-POM was measured in an open system during the same time and did not vary with day length (see "Results"). Thus, we assumed that the average $\delta^{13}C_{FA}$ value from p-POM during maximum ice extent for each 13 FA could be used to approximate the i-POM $\delta^{13}C_{FA}$ value when the fraction of the source reacted was zero (i.e., p-POM represents i-POM before isotopic discrimination results from the closed sea ice conditions). These values were used to calculate Δ for each FA ($\Delta$ = average $\delta^{13}C_{FA}$ of p-POM $-$ $\delta_{Source}$). The fraction reacted for each FA at a given day length was determined using the Solver Function in Microsoft Excel (version 14.3.2 for Mac 2011). Linear regression was performed

between day length and the fraction reacted for the 13 selected FAs to determine if day length could be used to predict the fraction of source reacted. The Mann–Whitney *U*-test, Kruskal–Wallis ANOVA, Spearman's rank order correlations and linear regression were performed using Statistica version 12 (StatSoft).

## Results

### FA content

The FA profile from the sample from the deep basin was different than that of other samples collected over the Bering Sea shelf during ice melt (Fig. 2), and because the station from the deep basin did not experience ice cover it was not included in further data analyses. FA profiles were significantly different between i-POM and p-POM, and also varied seasonally within p-POM (Fig. 2; PERMANOVA, $P = 0.001$). Average dissimilarity between i-POM and p-POM FA profiles during maximum ice extent was 31.8 % (SIMPER) with the diatom FAs 16:4n-1 and 20:5n-3 contributing most to the dissimilarity (7.1 and 5.9 %, respectively). These two FAs were present in greater proportions in i-POM (16:4n-1, 6.6–8.7 %; 20:5n-3, 19.6–25.9 %) than in p-POM (16:4n-1, 1.2–4.0 %; 20:5n-3, 5.5–14.0 %). i-POM samples collected during maximum ice extent had lower proportions of 14:0, 16:0, 16:1n-7 and 20:5n-3, and higher proportions of

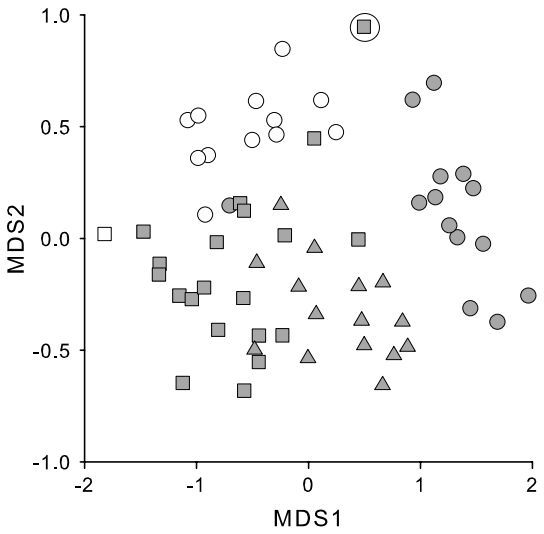


**Fig. 2** Non-metric multidimensional scaling (*MDS*) plot of i-POM (*open symbols*) and p-POM (*shaded symbols*) using 59 fatty acids (FAs) present in proportions >0.1 % in samples collected in 2010 during maximum ice extent (*circles*; i-POM $n = 12$, p-POM $n = 14$), ice melt (*squares*; i-POM $n = 1$, p-POM $n = 20$), and ice-free (*triangles*; p-POM $n = 15$) conditions from all stations; data from the deep basin station are *circled* (two-dimensional stress = 0.09). For other abbreviations, see Fig. 1

18:0, 16:1n-11, 18:1n-9, 18:1n-7, 20:1n-7, 16:4n-1, 18:4n-3 and 22:6n-3 compared to the *M. arctica* sample collected during ice melt (Fig. 3). Within p-POM, FA profiles were most dissimilar between maximum ice and ice melt conditions (33.7 %, SIMPER). Dissimilarity during maximum ice and ice-free conditions, and ice melt and ice-free conditions was 27.1 and 23.0 %, respectively. FA profiles of p-POM also showed some seasonal patterns with proportions of 16:1n-9, 18:0, 18:1n-9, 20:1n-7 and 22:1n-9 being relatively higher during maximum ice extent, lower during ice melt, and higher again during ice-free conditions. Proportions of 22:6n-3 in p-POM increased seasonally (Fig. 3). Total amounts of saturated FA (SAT), monounsaturated FA (MUFA), and polyunsaturated FA (PUFA) varied by POM type and seasonally within p-POM (Fig. 3). The amount of SAT from i-POM (22.0–26.3 %) was lower than that from p-POM (26.8–34.9 %). During maximum ice extent and ice melt conditions, levels of MUFA from i-POM were also lower (31.3–32.0 %) than from p-POM (40.6–42.3 %). In contrast, the amount of PUFA from i-POM (41.9–43.8 %) was higher than that from p-POM (18.6–34.8 %).

Diatom biomarkers (16:1/16:0, 16:4n-1) were higher than the dinoflagellate biomarker (22:6n-3/20:5n-3) in i-POM (Fig. 4a). This was also observed in p-POM samples during ice melt. However, in p-POM the levels of 16:4n-1 were lower than in i-POM and the ratios of 16:1/16:0 and 22:6n-3/20:5n-3 were similar in p-POM samples during maximum ice extent and ice-free conditions (Fig. 4a). The bacterial indicator (i.e., the sum of 15:0, 17:0, and the iso- and anteiso FA) was <4 % of the total FAs in all POM samples (Fig. 4b). However, the concentration of the bacterial indicator in the bottom 1 cm of sea ice ranged from 14 to 245 $\mu g\ L^{-1}$, which was on average 115 times greater than the bacterial indicator in the water column during maximum ice extent. The concentrations of the bacterial indicator in the water column during maximum ice extent, ice melt, and ice-free conditions were $0.6 \pm 0.3$, $1.7 \pm 0.8$, $0.6 \pm 0.2\ \mu g\ L^{-1}$ (mean ± SD), respectively.

In March 2010, total concentrations of FAs in the bottom 1 cm of sea ice ranged from 721 to 28,000 $\mu g\ L^{-1}$, which was 60 to almost 1,000 times greater than concentrations measured in the water column (8–542 $\mu g\ L^{-1}$). FA concentrations in the water column showed seasonal change with the highest concentrations measured during ice melt in all FA except for 18:1n-9 (Fig. 5). Concentrations of n-3 and n-6 PUFA in the bottom 1 cm of sea ice ranged from 123 to 9,500 and 42–732 $\mu g\ L^{-1}$, respectively. These values were also higher than those found in the water column (n-3 PUFA, 2.9–29.6 $\mu g\ L^{-1}$; n-6 PUFA, 0.8–2.3 $\mu g\ L^{-1}$). FA concentrations in the bottom 1 cm of sea ice increased with day length for all FAs ($R^2 > 0.48$), except 18:1n-9 ($R^2 = 0.16$, Spearman's $P = 0.60$). FA concentrations also increased with increasing POC and chlorophyll a concentrations measured in the bottom 1 cm of sea ice ($R^2 > 0.48$).

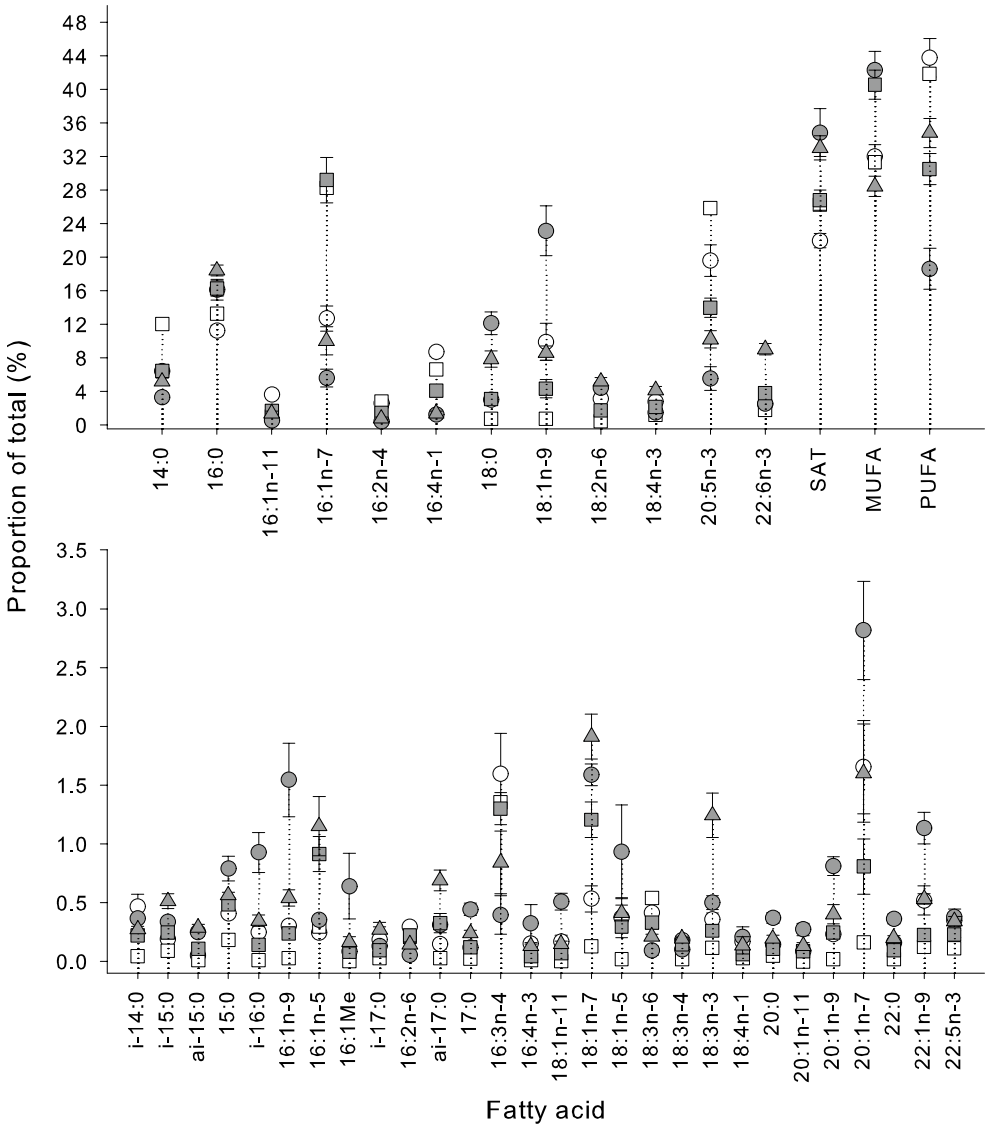


**Fig. 3** Proportions of some FAs (mean ± SE) in i-POM (*open symbols*) and p-POM (*shaded symbols*) collected in 2010 during maximum ice extent (*circles*; i-POM $n = 12$, p-POM $n = 14$), ice melt (*squares*; i-POM $n = 1$, p-POM $n = 20$), and ice-free (*triangles*; p-POM $n = 15$) conditions. For abbreviations, see Figs. 1 and 2

## $\delta^{13}C_{FA}$ values

The $\delta^{13}C_{FA}$ values of 13 selected FA varied between POM types and among seasonal p-POM samples (Fig. 6). During maximum ice extent, $\delta^{13}C_{FA}$ values from i-POM were higher compared with those from p-POM (Mann–Whitney *U*-test, $P < 0.05$; difference between means ranging from 1.2 to 7.9 ‰), with the exception of 16:2n-4, 16:3n-4, 16:4n-1, and 18:1n-9. Within p-POM samples, $\delta^{13}C_{FA}$ values were significantly different among ice regimes for 18:0 and the unsaturated FAs 16:3n-4, 18:1n-9, 18:2n-6, and 18:4n-3 (Kruskal–Wallis ANOVA, $P < 0.04$; Fig. 6). The $\delta^{13}C_{FA}$ values from i-POM increased with increasing day length for all FAs measured (Fig. 7a). Correlations between $\delta^{13}C_{FA}$ values of i-POM and day length were significant ($R^2 > 0.73$, Spearman's $P < 0.01$) for all FAs except for 18:1n-9 ($R^2 = 0.50$, Spearman's $P = 0.60$). We found no correlation between $\delta^{13}C_{FA}$ values of the 13 selected FAs in p-POM and day length during maximum ice extent and ice melt conditions (Spearman's $P > 0.05$). Only the $\delta^{13}C_{FA}$ value of 22:6n-3 ($R^2 = -0.73$, Spearman's $P = 0.003$) in p-POM decreased significantly with day length during ice-free conditions.

POC concentration and bulk $\delta^{13}C$ values measured in i-POM during maximum ice extent significantly increased with day length (Spearman's $R^2 > 0.66$, $P < 0.03$). In p-POM,

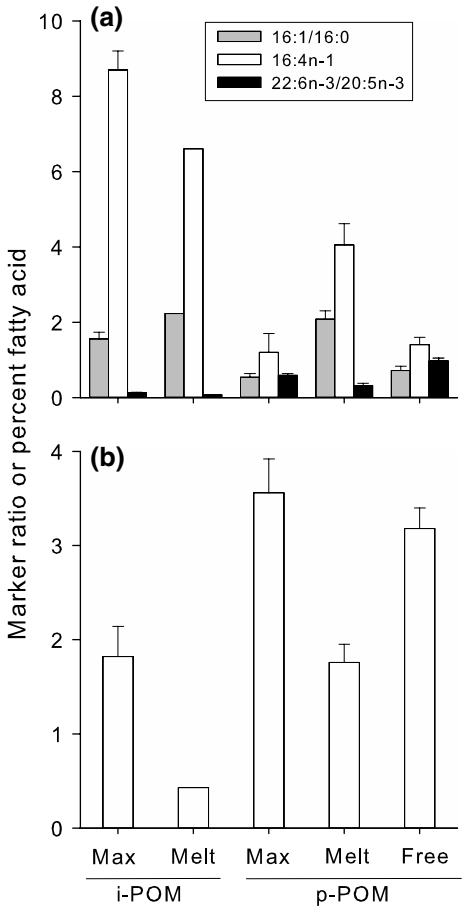


**Fig. 4** **a** Diatom FA indicators 16:1/16:0, 16:4n-1, and dinoflagellate indicator 22:6n-3/20:5n-3 and **b** bacterial FA indicator (sum of 15:0, 17:0 and all iso- and anteiso-branched chain FAs) in i-POM and p-POM collected during maximum ice extent (*Max*; i-POM $n = 12$, p-POM $n = 14$), ice melt (*Melt*; i-POM $n = 1$, p-POM $n = 20$), and ice-free (*Free*; p-POM $n = 15$) conditions (mean ± SE). For other abbreviations, see Figs. 1 and 2

only the concentration of 22:6n-3 significantly increased with day length (Spearman's $R^2 = 0.45$, $P = 0.002$). The average fractionation ($\Delta$) between ocean water DIC and i-POM during maximum ice extent for the 13 selected FAs ranged from 26.6 to 33.9 ‰ and the percentage of DIC assimilated into FA synthesis at the longest day ranged from 12 to 73 % (Fig. 8). Day length and fraction reacted were significantly positively correlated for all FAs ($P < 0.02$), except for 18:1n-9 (Spearman's $R^2 = 0.41$, Fig. 8).

## Discussion

### FA content

The FA biomarkers indicated that the relative amounts of diatoms, dinoflagellates, and bacteria in i-POM differed from those in p-POM and changed seasonally within p-POM. Although algal species were not identified in these samples, the algal class composition of POM can be partially inferred using FA biomarkers (reviewed in Dalsgaard et al. 2003). Using 16:4n-1 and the ratio of 16:1/16:0 as diatom biomarkers and the ratio of 22:6n-3/20:5n-3 as a dinoflagellate biomarker, i-POM during maximum ice extent appears to be dominated by diatoms, as is typical for Arctic sympagic communities (Horner 1985; Gradinger 2002; Arrigo et al. 2010). The ratios of the diatom marker 16:1/16:0 in the i-POM sampled during maximum ice extent, the *M. arctica* sampled during ice melt, and also the p-POM sampled during ice melt had similar values to those found in ice algae (2.7) and phytoplankton (2.3) from the Chukchi region (Budge et al. 2008). Additionally, the FA composition of the *M. arctica* sampled during ice melt confirmed that these FA ratios are a good diatom indicator in Arctic sea ice. In comparison, the ice algae sample from Budge et al. (2008), which was dominated by the pennate diatom *Navicula* sp., contained almost twice as much of the diatom marker 16:1n-7 (50.0 %) and approximately three times less of diatom markers 16:4n-1 (2.1 %) and 20:5n-3 (9.6 %) than our centric diatom *M. arctica* sample. Proportions of other FAs were similar between our *M. arctica* sample and the *Navicula* sp. samples from Budge et al. (2008). Different diatom species can produce different proportions of FA (i.e., Viso and Marty 1993, Dunstan et al. 1994). Thus, species differences may explain the striking differences in the three diatom markers (16:1n-7, 16:4n-1, and 20:5n-3) in the proportions of some FAs between our *M. arctica* sample and the *Navicula* sp. samples from Budge et al. (2008). Differences in environmental conditions between the Bering and Chukchi Seas at the time of sampling may have also contributed to the differences in FA profiles between these two diatom species as temperature, nutrient, and light availability are known to influence phytoplankton FA composition (Harrison et al. 1990; Thompson et al. 1992; Leu et al. 2010).

The relative abundance of diatom marker 16:4n-1 from p-POM taken during maximum ice extent was almost an order of a magnitude lower than that of i-POM, which could indicate lower diatom abundance in p-POM under heavy ice conditions or that concentrations of diatom FAs in p-POM were lower than in i-POM. The relative amounts of diatom markers 16:1/16:0 and 16:4n-1 for p-POM doubled in amount during ice melt compared with those measured during maximum ice extent. The presence of diatoms in p-POM during ice melt was confirmed by the observation of diatoms such as *Thalassiosira* sp., *N. frigida*, *Fragilariopsis* sp., *Chaetoceros* sp., and *Pseudo-nitzschia* sp., in these p-POM samples, with only three of 21 stations having notable amounts of the prymnesiophyte *Phaeocystis* (K. Iken, personal observation). Furthermore,

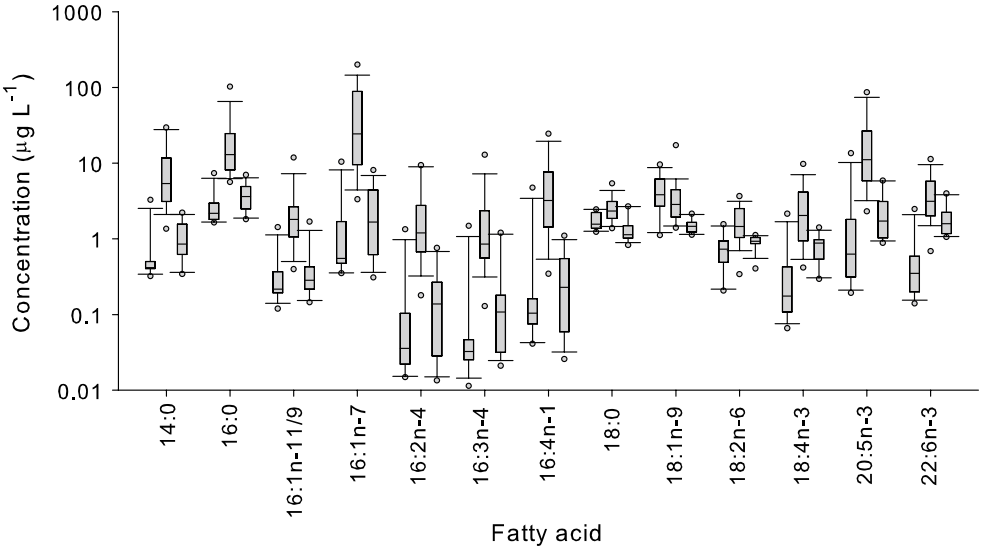


**Fig. 5** Boxplot of concentrations of 13 FAs in the water column. For each FA, the *first boxplot* represents maximum ice extent ($n = 14$), the *second* ice melt ($n = 20$), and the *third* ice-free conditions ($n = 15$). *Ends* of the boxes define the 25th and 75th percentiles, the *line* is at the median, the *whiskers* define the 10th and 90th percentiles, and the *circles* represent outliers. Note log scale used on *y*-axis

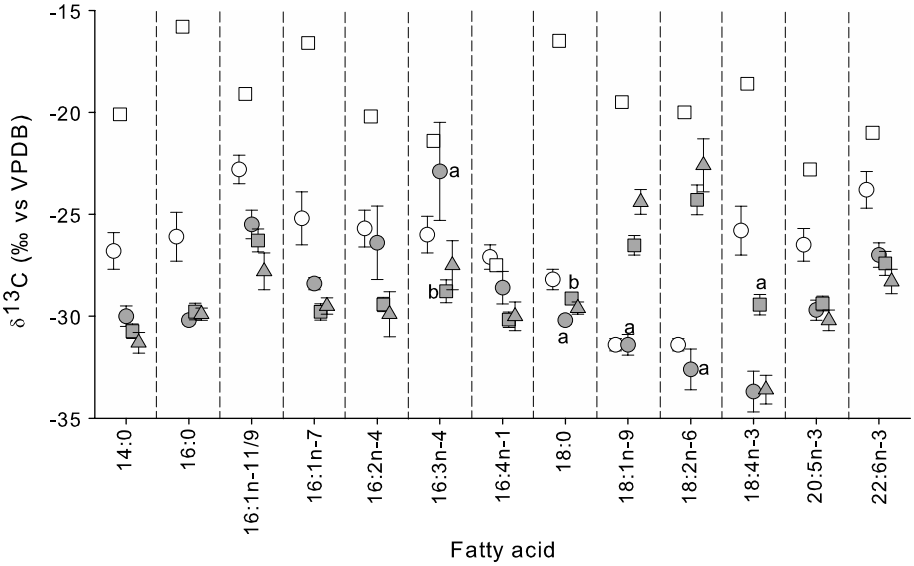


**Fig. 6** $\delta^{13}C_{FA}$ values for 13 select FAs (mean ± SE) in i-POM (*open symbols*) and p-POM (*shaded symbols*) samples during maximum ice extent (*circles*; i-POM $n = 10$–12, p-POM $n = 3$–12), ice melt (*squares*; i-POM $n = 1$, p-POM $n = 14$–20), and ice-free (*triangles*; p-POM $n = 1$–14) conditions in 2010. Sample sizes are given as ranges because not all FAs were present in sufficient quantities to be analyzed by gas chromatography–isotope ratio mass spectrometry in each sample. These 13 FAs were identified in the majority of the samples (63–100 %). *Different letters* indicate differences between values within p-POM (Kruskal–Wallis ANOVA, $P < 0.04$). *VPDB* Vienna Pee Dee Belemnite; for other abbreviations, see Figs. 1 and 2

the relative proportions of 16:0, 18:0, 16:1n-7, 18:1n-9, 18:1n-7, 20:1n-11, 20:1n-9, 20:1n-7, 16:4n-1, 20:5n-3, and 22:6n-3 in p-POM during ice melt are very similar to those found in the pelagic phytoplankton samples from Budge et al. (2008), which comprised mainly of the large centric diatom *Coscinodiscus* sp. This similarity also suggests that the p-POM samples during ice melt contained diatoms. The diatom species present during maximum ice extent are unknown but the diatom marker FAs during that time was much lower than during ice melt. The relative amounts of diatom markers 16:1/16:0 and 16:4n-1 for p-POM were lowest during maximum ice extent and ice-free conditions,

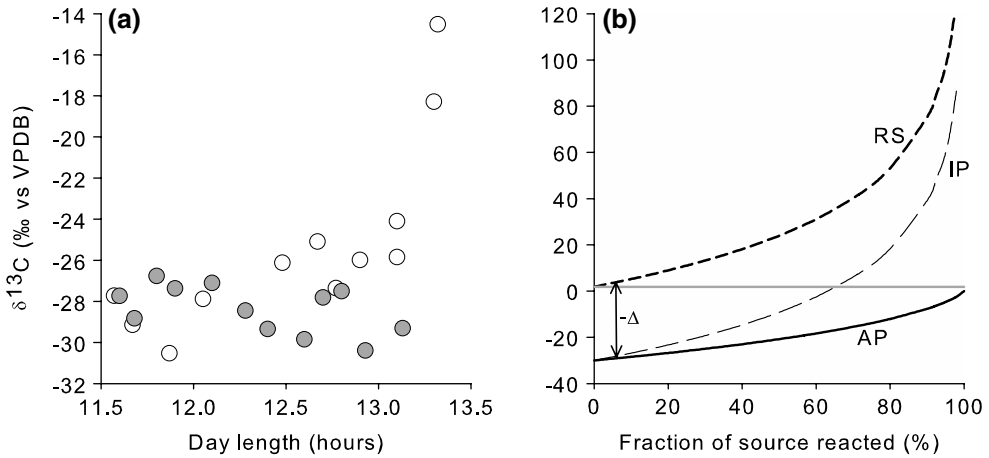


**Fig. 7** **a** Day length and $\delta^{13}C_{FA}$ values for FA 16:1n-7 in i-POM (*open symbols*, $n = 12$) and p-POM (*shaded symbols*, $n = 12$) during maximum ice extent conditions in 2010. Spearman's rank correlations for all other i-POM FAs and day length were significant except for 18:1n-9; **b** isotopic fractionation (Δ) in a closed system. Δ is the difference between the residual substrate (*RS*) and instantaneous product (*IP*). In a closed system such as sea ice habitat, the source is ocean dissolved inorganic carbon [*shaded horizontal line* at 1.85 ‰ (Gruber et al. 1999)] and the accumulated product (*AP*) is measured i-POM. For other abbreviations, see Figs. 1, 2 and 6

and highest during ice melt while the dinoflagellate indicator 22:6n-3/20:5n-3 showed the opposite pattern. This seasonal change in dominance of diatoms is consistent with a succession of taxa from low levels of primary production during maximum ice extent limited by light and stratification, transitioning to a water column seeded by diatoms released from sea ice as it melted during a spring bloom (McRoy and Goering 1974; Alexander and Niebauer 1981; Jin et al. 2007). When the ice retreats in the Bering Sea, the diatom bloom community can be succeeded by non-diatom phytoplankton such as dinoflagellates, haptophytes such as *Phaeocystis* sp., and *Synechococcus* sp., and cryptophytes (Moran et al. 2012). Although 22:6n-3/20:5n-3 has been historically used as a dinoflagellate indicator because 22:6n-3 can be produced in large amounts by dinoflagellates, 22:6n-3 can also be biosynthesized by heterotrophic flagellates (e.g., Desvilettes and Bec 2009, Bec et al. 2010). Therefore, it is possible that an increase in 22:6n-3/20:5n-3 of p-POM from ice melt to ice-free conditions may be due to a shift toward a stronger microbial food web with heterotrophic protists. The increased contribution of bacteria to p-POM is further supported by the increase in the bacterial biomarkers in the water column during ice melt to ice-free conditions (see below). Most likely the increase in 22:6n-3/20:5n-3 reflects a combination of increased dinoflagellate production with concurrent decreases in diatom production, as well as contributions from heterotrophic protists that can synthesize 22:6n-3 from other FA precursors such as 20:5n-3.

The proportion of bacterial FA markers indicates the presence of bacteria in POM, and the concentration of this marker suggests a greater total abundance of bacteria in the bottom 1 cm of sea ice than in the water column. In fact, bacteria can contribute up to 50 % of the total biomass within sea ice (Gradinger and Zhang 1997) and can be up to 100 times greater in abundance in Arctic sea ice relative to the water column (Maranger et al. 1994). In comparison, the bacterial FA marker in ice algae from the Chukchi region (1.4 %) was lower than that found in i-POM during maximum ice extent and higher than the bacterial marker in *M. arctica*. The bacterial FA marker in pelagic phytoplankton from the Chukchi region (0.9 %) was lower than those in p-POM (1.8–3.6 %), indicating a higher relative contribution of bacteria in p-POM. In addition to algae and bacteria, the POM samples most likely contained small amounts of detritus and microzooplankton that may have influenced FA profiles of these samples. Within sea ice, meiofauna typically contribute a minor fraction to total biomass and heterotrophic flagellates can be an important source of carbon (Gradinger et al. 1999). However, the FA profiles of i-POM and p-POM (during ice melt) were similar to those found in pure ice algae and pelagic phytoplankton from the Chukchi Sea (Budge et al. 2008); therefore, the presence of material other than algae is likely negligible.

In addition to the differences and seasonal changes in community composition of POM in the Bering Sea, the nutritional quality (i.e., levels of PUFA) of POM within sea ice and the water column also varied, as well as seasonally within the water column. Seasonal increase of FA concentrations within the water column during ice melt could be explained by an increase of phytoplankton cells during the spring bloom or from ice algae being released into the water column. The diatom FA biomarkers 16:1/16:0 and 16:4n-1 suggest that the increases in relative proportions of

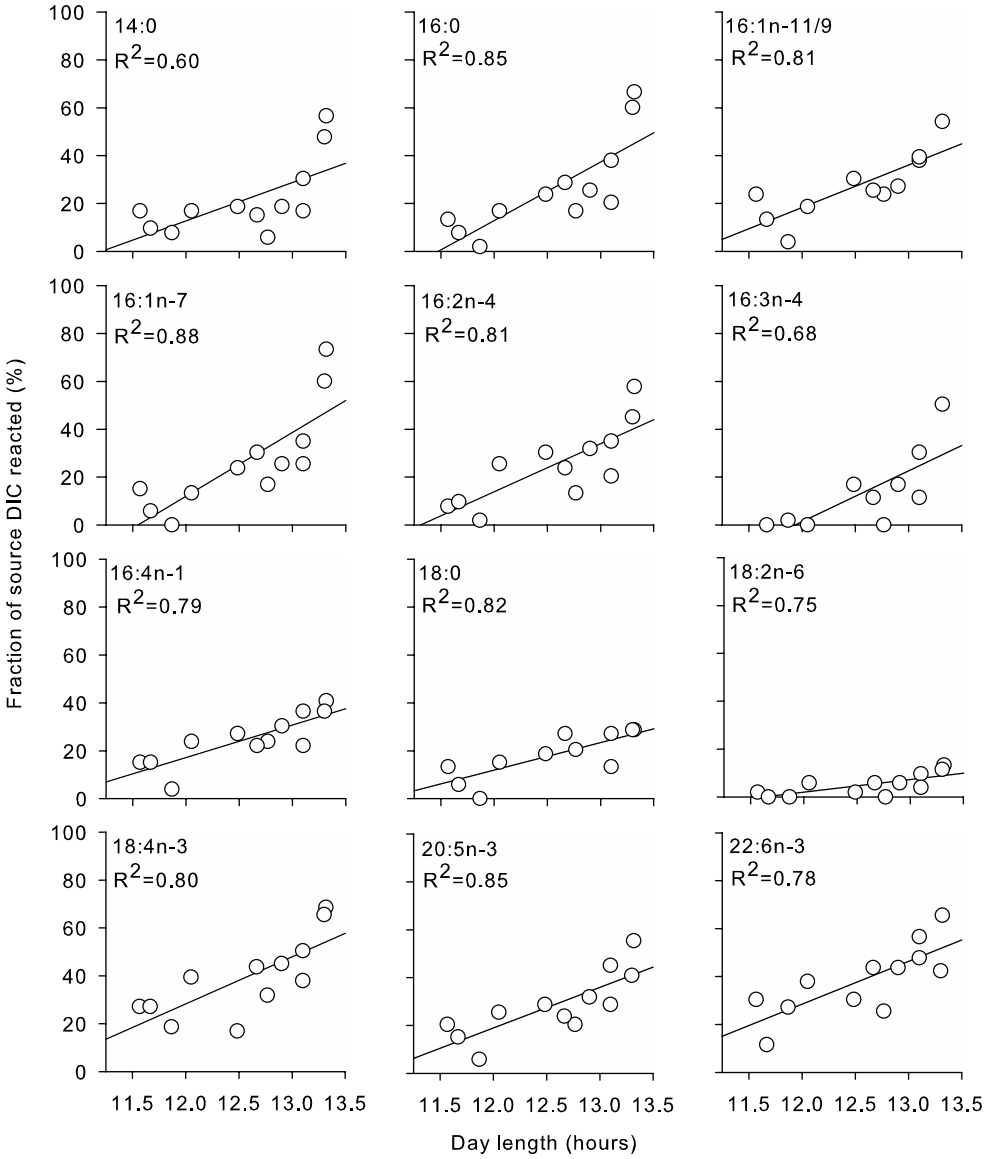


**Fig. 8** Day length and fraction of source dissolved inorganic carbon (*DIC*) reacted for 12 FAs of i-POM during maximum ice extent conditions in 2010. For all FA $n = 12$, except for 16:1n-11/9 ($n = 11$), 16:3n-4 ($n = 10$), and 18:0 ($n = 11$). Results shown for a source DIC value of 1.85 ‰ (Gruber et al. 1999). Results from using a value of 1.55 ‰ from Quay et al. (2003) gave similar results that could not be distinguished in the figure. Linear regressions were significant for all FA shown ($P < 0.02$). Data for 18:1n-9 not shown because they were not significant. For other abbreviations, see Figs. 1 and 2

FAs in p-POM during ice melt are largely from the release of i-POM. However, if p-POM during ice melt was largely influenced by sinking i-POM we might expect the $\delta^{13}C_{FA}$ of p-POM to be similar to that of i-POM, but this is not the case. It is likely that the p-POM during ice melt is influenced by both the sinking of i-POM and active p-POM production in the water column. The concentrations of n-3 and n-6 PUFA in the bottom 1 cm of sea ice ranged from 40 to almost 300 times greater than those measured in the water column. The higher PUFA levels in sea ice compared to the water column indicated that the material in the bottom 1 cm of sea ice has a higher, concentrated, nutritional value than that of material in the water column, likely making the sea ice habitat an important, concentrated source of PUFA for grazers (e.g., Falk-Petersen et al. 1998) and presumably for higher trophic levels (e.g., Bluhm et al. 2010). For example, the Arctic bivalve *Macoma balthica* preferentially consumed sea ice algae over phytoplankton, and both *M. balthica* and the amphipod *Monoporeia affinis* had higher levels of PUFA and total FAs when fed on sea ice algae compared to phytoplankton (Sun et al. 2009). Thus, these two Arctic benthic species may provide an important source of PUFA for animals that consume them. A similar observation was noted in the copepod *Calanus glacialis* in Rijpfjorden, Svalbard, Norway where its FA composition indicated that sea ice algae were an important food source during the spring bloom, when ice algae, not pelagic algae, triggered the reproduction of zooplankton (Leu et al. 2011). It may be that sea ice algae are preferentially eaten by some consumer taxa simply because they are present in larger concentrations than phytoplankton when released from the sea ice (e.g., Carroll and Carroll 2003). However, higher

ice algal concentrations would also provide greater concentrations of PUFA to consumers.

## $\delta^{13}C_{FA}$ values

In addition to differences in FA profiles between i-POM and p-POM, and variances in the nutritional content between sea ice and the water column, our data suggest that there are fundamental differences in the processes influencing FA production in the sympagic versus pelagic habitat. Overall, most of the 13 FAs from i-POM analyzed for their $\delta^{13}C$ were more enriched in $^{13}C$ compared to p-POM, including the diatom biomarkers 16:4n-1 and 20:5n-3. These results agree with some previous bulk and compound-specific carbon stable isotope analyses of sea ice algae and i-POM that have shown them to be more enriched in $^{13}C$ than pelagic phytoplankton and p-POM (Hobson et al. 1995; Gibson et al. 1999; Søreide et al. 2006, 2013; Budge et al. 2008; Tamelander et al. 2008). This implies that isotopic reaction processes during FA production differ markedly between the sympagic and pelagic environments in which the FAs were synthesized. The i-POM $\delta^{13}C_{FA}$ values increased with increasing day length, while the $\delta^{13}C_{FA}$ values from p-POM generally showed relatively little variation with increasing light availability during the same sampling period. We suggest that these patterns are consistent with a substantial influence of the photosynthetic isotope effect on FA production of i-POM from a limited DIC substrate within the semi-closed/closed sympagic system (Kennedy et al. 2002; Papadimitriou et al. 2007). These relatively higher photosynthetic demands within sea ice force decreased $^{13}C$ discrimination during photosynthesis and the subsequent increase in $\delta^{13}C_{FA}$ values in sympagic FAs, while pelagic production can draw from a constantly renewed DIC pool.

Patterns observed in $\delta^{13}C_{FA}$ values with increasing day length in the two POM types during maximum ice extent allow reaction progress associated with FA synthesis in sea ice to be inferred. Firstly, the $\delta^{13}C_{FA}$ values for many of the FAs of i-POM and p-POM were similar at the lowest day length, which is an indication of the baseline fractionation associated with FA synthesis relative to source DIC. Secondly, the $\delta^{13}C_{FA}$ values of p-POM FAs were relatively invariable over the light availability gradient, which is consistent with FA synthesis by primary production in an open system where source DIC is constantly being replenished. Thirdly, bulk $\delta^{13}C$ values measured in i-POM increased, as did the $\delta^{13}C_{FA}$ values for many of the sympagic FAs, with increased light availability, which is consistent with a reaction progress in a closed system (e.g., Fry 2006). Finally, the $\delta^{13}C_{FA}$ values of many of the sympagic FAs differed under the highest light conditions relative to typical marine DIC values, which implies that the fraction of the source reacted increased with increasing day length, but reaction progress did not go to completion. In other words, when the reaction progress is complete, the $\delta^{13}C_{FA}$ value of i-POM should equal that of the initial $\delta^{13}C$ value of source DIC (Fry 2006). The estimated 12–73 % of source DIC reacted indicated that in the semi-closed/closed sea ice system, DIC was not completely limiting and was still available for FA synthesis.

There are many factors that, in combination, contribute to the variability in our estimates of reaction progress among sympagic FAs. One source of variability could be that synthesis pathways may be different for the various FAs analyzed. On average, SAT and PUFA gave similar estimates of reaction progress (51 and 50 %, respectively) while, overall, MUFA gave a higher estimate of reaction progress (64 %). This may reflect the activities of different desaturase enzymes used to insert bonds versus elongation enzymes used to add carbon to FAs. Another source of variability in reaction progress estimates could stem from the $\delta^{13}C$ values for surface water DIC. The $\delta^{13}C$ values for surface water DIC in the Bering Sea are not available, therefore, we used values estimated for the entire Pacific Ocean and also from the Gulf of Alaska (Gruber et al. 1999; Quay et al. 2003), which may not reflect the true value for our study area. However, the range of source DIC $\delta^{13}C$ values we used provided very similar estimates of fraction of source DIC reacted. We suggest that additional factors besides day length may also influence reaction progress estimates for sympagic FA synthesis (i.e., nutrient availability, brine convection, internal carbon mineralization). An incomplete reaction progress could also be due to sampling time, i.e., day length at the time of sampling may not have been great enough. Replenishment of the DIC pool could also lead to an incomplete reaction progress. This could also occur from the recycling of carbon from the breakdown of organic matter within sea ice and if the sympagic system was a semi- rather than a fully closed system. The most parsimonious explanation is that ice breakup occurs before the reaction of DIC can go to completion, and there is insufficient time to exhaust the DIC pool within sea ice. Further research is needed to determine if $\delta^{13}C_{FA}$ values of POM vary regionally and annually, and what factors may influence reaction progress estimates for sympagic FA synthesis.

## Conclusion

In summary, we found differences in FA profiles and $\delta^{13}C_{FA}$ values between i-POM and p-POM and seasonally within p-POM. We demonstrated that these results can be explained as differences and changes in the composition of diatoms, flagellates, and bacteria using FA biomarkers. Concentrations of FA within the bottom 1 cm of sea ice were much greater than those found in the water column,

making the sea ice a concentrated source of PUFA for marine grazers. In i-POM, the FAs became more enriched in $^{13}C$ with increasing day length, and we suggest that the decreased isotopic discrimination during photosynthesis in the carbon-limited and semi-closed sympagic habitat influences this pattern. Finally, we estimated that between 12 and 73 % of sea water DIC was used for FA synthesis in i-POM.

The marked differences in diatom versus flagellate composition in sympagic and pelagic community POM in 2010 and the higher nutritional content within the bottom 1 cm of sea ice compared to within the water column may have implications for marine grazers and possibly higher trophic levels. Of the regions in the Arctic and sub-Arctic, the Bering Sea exhibits the largest seasonal sea ice advance and retreat (Walsh and Johnson 1979; Niebauer 1983; Minobe 2002; Bluhm and Gradinger 2008). By 2050, the spring sea ice extent in the eastern Bering Sea is predicted to be 58 % of the 1980–1999 mean (Wang et al. 2012). As a result of this overall loss of sea ice and early ice retreat due to climate change, a reduction of sea ice primary productivity is predicted to occur (e.g., Bluhm and Gradinger 2008). Additionally, climate-related changes in the timing of seasonal sea ice cover affect spring primary production patterns (Stabeno et al. 2001, 2010; Hunt and Stabeno 2002). These changes in timing of sea ice retreat, predicted loss of sea ice and sea primary productivity, along with increased light intensities may lead to a reduction in high-quality PUFA from i-POM available for sympagic marine organisms and could have profound effects on ice-associated fauna, and possibly on upper trophic level consumers that rely on them as a food resource. The characteristics of FA in i-POM and differences from p-POM elucidated in our study will aid efforts to track the quantitative importance of sea ice algae FA to higher trophic levels in the Bering Sea.

**Acknowledgments** This project was funded by the National Science Foundation (ARC-0902177 and 0732767). Financial support for S. Wang was also provided by the North Pacific Research Board Graduate Research Award, the University of Alaska Center (UAF) for Global Change Student Research Grant with funds from the Cooperative Institute for Alaska Research, Robert Byrd Award, Dieter Family Marine Science Research Scholarship, and the Ken Turner Memorial Fellowship. We thank J. Weems and S. Brennan (UAF) for assisting with sample collections and A. Timmins (Dalhousie) for laboratory assistance. We also thank T. Howe, N. Haubenstock, C. Graham from the ASIF-UAF for laboratory assistance with stable isotope analyses. We are grateful for the excellent assistance of the crew and captains of the USCGC Polarsea and the UNOLS vessel Thomas G. Thompson, and chief scientists L. Cooper (University of Maryland Center for Environmental Science), C. Ashjian (Woods Hole Oceanographic Institution), and D. Shull (Western Washington University). We also thank E. Lessard (University of Washington) for assistance with phytoplankton identifications. Sea ice concentration data were sourced from the model explorer provided by the Alaska Ocean Observing System. Finally, we thank D. O'Brien, L. Horstmann-Dehn, A. Springer, and L. Oxtoby for helpful discussions and comments, and three anonymous reviewers for their detailed and constructive comments which improved our manuscript.

## References

Abrajano TA, Murphy DE, Fang J, Comet P (1994) $^{13}C/^{12}C$ ratios in individual fatty acids of marine mytilids with and without bacterial symbionts. Org Geochem 21:611–617

Alexander V, Niebauer HJ (1981) Oceanography of the eastern Bering Sea ice-edge zone in spring. Limnol Oceanogr 26:1111–1125

Anderson MJ (2001) A new method for non-parametric multivariate analysis of variance. Aust Ecol 26:32–46

Arrigo KR, Mock T, Lizotte MP (2010) Primary producers and sea ice. In: Thomas DN, Dieckmann GS (eds) Sea ice. Wiley-Blackwell, Oxford, pp 283–325

Auel H, Harjes M, da Rocha R, Stübing D, Hagen W (2002) Lipid biomarkers indicate different ecological niches and trophic relationships of the Arctic hyperiid amphipods *Themisto abyssorum* and *T. libellula*. Polar Biol 25:374–383

Bec A, Martin-Creuzburg D, Von Elert E (2010) Fatty acid composition of the heterotrophic nanoflagellate *Paraphysomonas* sp.: influence of diet and de novo biosynthesis. Aquat Biol 9(107):112

Bluhm BA, Gradinger R (2008) Regional variability in food availability for Arctic marine mammals. Ecol Appl 18:S77–S96

Bluhm BA, Gradinger RR, Schnack-Schiel SB (2010) Sea ice meio- and macrofauna. In: Thomas DN, Dieckmann GS (eds) Sea ice. Wiley-Blackwell, Oxford, pp 357–393

Budge SM, Parrish CC (1998) Lipid biogeochemistry of plankton, settling matter and sediments in Trinity Bay, Newfoundland. II. Fatty acids. Org Geochem 29:1547–1559

Budge SM, Iverson SJ, Koopman HN (2006) Studying trophic ecology in marine ecosystems using fatty acids: a primer on analysis and interpretation. Mar Mammal Sci 22:759–801

Budge SM, Springer AM, Iverson SJ, Sheffield G (2007) Fatty acid biomarkers reveal niche separation in an Arctic benthic food web. Mar Ecol Prog Ser 336:305–309

Budge SM, Wooller MJ, Springer AM, Iverson SJ, McRoy CP, Divoky GJ (2008) Tracing carbon flow in an Arctic marine food web using fatty acid-stable isotope analysis. Oecologia 157:117–129

Carroll ML, Carroll J (2003) The Arctic seas. In: Black KD, Shimmield GB (eds) Biogeochemistry of marine systems. CRC, Boca Raton, pp 127–156

Cavalieri DJ, Parkinson CL, Gloersen P, Zwally H (1996, updated yearly) Sea ice concentrations from Nimbus-7 SMMR and DMSP SSMI/I-SSMIS passive microwave data. 2010. NASA DAAC at the National Snow and Ice Data Center, Boulder, CO

Clarke KR (1993) Non-parametric multivariate analyses of changes in community structure. Aust J Ecol 18:117–143

Claustre H, Marty J-C, Cassiani L, Dagaut J (1988/1989) Fatty acid dynamics in phytoplankton and microzooplankton communities during a spring bloom in the coastal Ligurian Sea: ecological implications. Mar Microb Food Webs 3:51–66

Cooper LW, Sexson MG, Grebmeier JM, Gradinger R, Mordy CW, Lovvorn JR (2013) Linkages between sea-ice coverage, pelagic–benthic coupling, and the distribution of spectacled eiders: Observations in March 2008, 2009 and 2010, northern Bering Sea. Deep Sea Res II (in press)

Dalsgaard J, St. John M, Kattner G, Müller-Navarra D, Hagen W (2003) Fatty acid trophic markers in the pelagic marine environment. Adv Mar Biol 46:225–340

Dehn L-A, Sheffield G, Follmann E, Duffy L, Thomas D, O'Hara T (2007) Feeding ecology of phocid seals and some walrus in the Alaskan and Canadian Arctic as determined by stomach contents and stable isotope analysis. Polar Biol 30:167–181

Desvilettes C, Bec A (2009) Formation and transfer of fatty acids in aquatic microbial food webs: role of heterotrophic protists. In: Arts MT, Brett MT, Kainz MJ (eds) Lipids in aquatic ecosystems. Springer, New York, pp 25–42

Dunstan GA, Volkman JK, Barrett SM, Leroi JM, Jeffrey SW (1994) Essential polyunsaturated fatty acids from 14 species of diatom (Bacillariophyceae). Phytochem 35:155–161

Falk-Petersen S, Sargent JR, Henderson J, Hegseth EN, Hop H, Okolodkov YB (1998) Lipids and fatty acids in ice algae and phytoplankton from the Marginal Ice Zone in the Barents Sea. Polar Biol 20:41–47

Feder H, Iken K, Blanchard A, Jewett S, Schonberg S (2011) Benthic food web structure in the southeastern Chukchi Sea: an assessment using $\delta^{13}C$ and $\delta^{15}N$ analyses. Polar Biol 34:521–532

Fischer G (1991) Stable carbon isotope ratios of plankton carbon and sinking organic matter from the Atlantic sector of the Southern Ocean. Mar Chem 35:581–596

Folch J, Lees M, Sloane-Stanley GH (1957) A simple method for the isolation and purification of total lipids from animal tissues. J Biol Chem 226:497–509

Fry B (2006) Technical supplement 7B: derivations of closed system isotope equations. Stable isotope ecology. Springer, New York

Gibson JAE, Trull T, Nichols PD, Summons RE, McMinn A (1999) Sedimentation of 13C-rich organic matter from Antarctic sea-ice algae: a potential indicator of past sea-ice extent. Geology 27:331–334

Gradinger RR (2002) Sea ice microorganisms. In: Bitten G (ed) Encyclopedia of environmental microbiology. Wiley, Hoboken, pp 2833–2844

Gradinger R, Zhang Q (1997) Vertical distribution of bacteria in Arctic sea ice from the Barents and Laptev Seas. Polar Biol 17:448–454

Gradinger R, Friedrich C, Spindler M (1999) Abundance, biomass and composition of the sea ice biota of the Greenland Sea pack ice. Deep Sea Res II 46:1457–1472

Gradinger RR, Kaufman MR, Bluhm BA (2009) Pivotal role of sea ice sediments in the seasonal development of near-shore Arctic fast ice biota. Mar Ecol Prog Ser 394:49–63

Grebmeier JM (2012) Shifting patterns of life in the Pacific Arctic and sub-Arctic seas. Annu Rev Mar Sci 4:63–78

Grebmeier JM, Overland JE, Moore SE, Farley EV, Carmack EC, Cooper LW, Frey KE, Helle JH, McLaughlin FA, McNutt SL (2006) A major ecosystem shift in the northern Bering Sea. Science 311:1461–1464

Gruber N, Keeling CD, Bacastow RB, Guenther PR, Lueker TJ, Wahlen M, Meijer HAJ, Mook WG, Stocker TF (1999) Spatiotemporal patterns of carbon-13 in the global surface oceans and the oceanic suess effect. Global Biogeochem Cycles 13:307–335

Harrison PJ, Thompson PA, Calderwood GS (1990) Effects of nutrients and light limitation on the biochemical composition of phytoplankton. J Appl Phycol 2:45–56

Hobson K, Ambrose WJ, Renaud P (1995) Sources of primary production, benthic-pelagic coupling, and trophic relationships within the Northeast Water Polynya: insights from $\delta^{13}C$ and $\delta^{15}N$ analysis. Mar Ecol Prog Ser 128:1–10

Horner RA (1985) Taxonomy of sea ice microalgae. In: Horner RA (ed) Sea ice biota. CRC, Boca Raton, pp 147–158

Hunt GL, Stabeno PJ (2002) Climate change and the control of energy flow in the southeastern Bering Sea. Prog Oceanogr 55:5–22

Hunt GL Jr, Stabeno P, Walters G, Sinclair E, Brodeur RD, Napp JM, Bond NA (2002) Climate change and control of the southeastern Bering Sea pelagic ecosystem. Deep Sea Res II 49:5821–5853

Hunt GL, Coyle KO, Eisner LB, Farley EV, Heintz RA, Mueter F, Napp JM, Overland JE, Ressler PH, Salo S, Stabeno PJ (2011) Climate impacts on eastern Bering Sea foodwebs: a synthesis of new data and an assessment of the Oscillating Control Hypothesis. ICES J Mar Sci 68:1230–1243

Iken K, Bluhm B, Dunton K (2010) Benthic food-web structure under differing water mass properties in the southern Chukchi Sea. Deep Sea Res II 57:71–85

Jin MB, Deal C, Wang J, Alexander V, Gradinger R, Saitoh S, Iida T, Wan ZW, Stabeno P (2007) Ice-associated phytoplankton blooms in the southeastern Bering Sea. Geophys Res Lett 34:L06612

Kennedy H, Thomas DN, Kattner G, Haas C, Dieckmann GS (2002) Particulate organic matter in Antarctic summer sea ice: concentration and stable isotopic composition. Mar Ecol Prog Ser 238:1–13

Leu E, Wiktor J, Søreide JE, Berge J, Falk-Petersen S (2010) Increased irradiance reduces food quality of sea ice algae. Mar Ecol Prog Ser 411:49–60

Leu E, Søreide JE, Hessen DO, Falk-Petersen S, Berge J (2011) Consequences of changing sea-ice cover for primary and secondary producers in the European Arctic shelf seas: timing, quantity, and quality. Prog Oceanogr 90:18–32

Lewis RW (1969) The fatty acid composition of Arctic marine phytoplankton and zooplankton with special reference to minor acids. Limnol Oceanogr 14:35–40

Litzow MA, Bailey KM, Prahl FG, Heintz R (2006) Climate regime shifts and reorganization of fish communities: the essential fatty acid limitation hypothesis. Mar Ecol Prog Ser 315:1–11

Maranger R, Bird DF, Juniper SK (1994) Viral and bacterial dynamics in Arctic sea ice during the spring algal bloom near Resolute, N.W.T., Canada. Mar Ecol Prog Ser 111:121–127

Mayzaud P, Chanut JP, Ackman RG (1989) Seasonal changes of the biochemical composition of marine particulate matter with special reference to fatty acids and sterols. Mar Ecol Prog Ser 56:189–204

Mayzaud P, Boutoute M, Noyon M, Narcy F, Gasparini S (2013) Lipid and fatty acids in naturally occurring particulate matter during spring and summer in a high Arctic fjord (Kongsfjorden, Svalbard). Mar Biol 160:383–398

McArdle BH, Anderson MJ (2001) Fitting multivariate models to community data: a comment on distance-based redundancy analysis. Ecology 82:290–297

McRoy CP, Goering JJ (1974) The influence of ice on the primary productivity of the Bering Sea. In: Hood DW, Kelley EJ (eds) Oceanography of the Bering Sea with emphasis on renewable resources. University of Alaska Fairbanks, Fairbanks, pp 403–421

McRoy CP, Goering JJ (1976) Annual budget of primary production in the Bering Sea. Mar Sci Commun 2:266–267

Minobe S (2002) Interannual to interdecadal changes in the Bering Sea and concurrent 1998/99 changes over the North Pacific. Prog Oceanogr 55:45–64

Moran SB, Lomas MW, Kelly RP, Gradinger R, Iken K, Mathis JT (2012) Seasonal succession of net primary productivity, particulate organic carbon export, and autotrophic community composition in the eastern Bering Sea. Deep Sea Res II 65–70:84–97

Naidu AS, Cooper LW, Finney BP, Macdonald RW, Alexander C, Semiletov IP (2000) Organic carbon isotope ratios ($\delta^{13}C$) of Arctic Amerasian Continental shelf sediments. Int J Earth Sci 89:522–532

Niebauer HJ (1983) Multiyear sea ice variability in the eastern Bering Sea—an update. J Geophys Res Oceans Atmos 88:2733–2742

Papadimitriou S, Thomas DN, Kennedy H (2007) Biogeochemical composition of natural sea ice brines from the Weddell Sea during early austral summer. Limnol Oceanogr 52: 1809–1823

Parrish CC (1999) Determination of total lipid, lipid classes and fatty acids in aquatic samples. In: Arts MT, Wainman BC (eds) Lipids in freshwater ecosystems. Springer, New York, pp 4–12

Peters J, Tuschling K, Brandt A (2004) Zooplankton in the Arctic Laptev Sea—feeding ecology as indicated by fatty acid composition. J Plankton Res 26:227–234

Quay P, Sonnerup R, Westby T, Stutsman J, McNichol A (2003) Changes in the $^{13}C/^{12}C$ of dissolved inorganic carbon in the ocean as a tracer of anthropogenic $CO_2$ uptake. Global Biogeochem Cycles 17:1004

Reuss N, Poulsen L (2002) Evaluation of fatty acids as biomarkers for a natural plankton community. A field study of a spring bloom and a post-bloom period off West Greenland. Mar Biol 141:423–434

Richter-Menge J, Overland J (2010) Arctic report card 2010. http://www.arctic.noaa.gov/report10

Rieley G (1994) Derivatization of organic compounds prior to gas chromatographic-combustion-isotope ratio mass spectrometric analysis: identification of isotope fractionation processes. Analyst 119:915–919

Schubert CJ, Calvert SE (2001) Nitrogen and carbon isotopic composition of marine and terrestrial organic matter in Arctic Ocean sediments: implications for nutrient utilization and organic matter composition. Deep Sea Res I 48:789–810

Søreide JE, Hop H, Carroll ML, Falk-Petersen S, Hegseth EN (2006) Seasonal food web structures and sympagic-pelagic coupling in the European Arctic revealed by stable isotopes and a two-source food web model. Prog Oceanogr 71:59–87

Søreide JE, Carroll ML, Hop H, Ambrose WG, Hegseth EN, Falk-Petersen S (2013) Sympagic-pelagic-benthic coupling in Arctic and Atlantic waters around Svalbard revealed by stable isotopic and fatty acid tracers. Mar Biol Res 9:831–850

Stabeno PJ, Bond NA, Kachel NB, Salo SA, Schumacher JD (2001) On the temporal variability of the physical environment over the south-eastern Bering Sea. Fish Oceanogr 10:81–98

Stabeno P, Napp J, Mordy C, Whitledge T (2010) Factors influencing physical structure and lower trophic levels of the eastern Bering Sea shelf in 2005: sea ice, tides and winds. Prog Oceanogr 85:180–196

Sun M-Y, Clough LM, Carroll ML, Dai J, Ambrose WG Jr, Lopez GR (2009) Different responses of two common Arctic macrobenthic species (*Macoma balthica* and *Monoporeia affinis*) to phytoplankton and ice algae: will climate change impacts be species specific? J Exp Mar Biol Ecol 376:110–121

Tamelander T, Reigstad M, Hop H, Carroll ML, Wassmann P (2008) Pelagic and sympagic contribution of organic matter to zooplankton and vertical export in the Barents Sea marginal ice zone. Deep Sea Res II 55:2330–2339

Thomas DN, Papadimitriou S, Michel C (2010) Biogeochemistry of sea ice. In: Thomas DN, Dieckmann GS (eds) Sea ice. Wiley-Blackwell, Oxford, pp 425–468

Thompson PA, Gou M, Harrison PJ, Whyte JNC (1992) Effects of variation in temperature. II. On the fatty acid composition of eight species of marine phytoplankton. J Physcol 28:488–497

Viso A, Marty J (1993) Fatty acids from 28 marine microalgae. Prog Lipid Res 32:1521–1533

Walsh JE, Johnson CM (1979) An analysis of Arctic sea ice fluctuations, 1953–77. J Phys Oceanogr 9:580–591

Walsh JJ, McRoy CP (1986) Ecosystem analysis in the southeastern Bering sea. Cont Shelf Res 5:259–288

Wang M, Overland JE, Stabeno P (2012) Future climate of the Bering and Chukchi Seas projected by global climate models. Deep Sea Res II 65–70:46–57

Weems J, Iken K, Gradinger R, Wooller MJ (2012) Carbon and nitrogen assimilation in the Bering Sea clams *Nuculana radiata* and *Macoma moesta*. J Exp Mar Biol Ecol 430–431:32–42